Variation in climate sensitivity and feedback parameters during the historical period

Article

Published Version

CentAUR

Variation in climate sensitivity and feedback parameters during the historical period

J. M. Gregory[1,2] and T. Andrews[2]

[1]NCAS-Climate, University of Reading, Reading, UK, [2]Met Office Hadley Centre, Exeter, UK

Abstract We investigate the climate feedback parameter α (W m^{-2} K^{-1}) during the historical period (since 1871) in experiments using the HadGEM2 and HadCM3 atmosphere general circulation models (AGCMs) with constant preindustrial atmospheric composition and time-dependent observational sea surface temperature (SST) and sea ice boundary conditions. In both AGCMs, for the historical period as a whole, the effective climate sensitivity is ∼2 K ($\alpha \simeq 1.7$ W m^{-2} K^{-1}), and α shows substantial decadal variation caused by the patterns of SST change. Both models agree with the AGCMs of the latest Coupled Model Intercomparison Project in showing a considerably smaller effective climate sensitivity of ∼1.5 K ($\alpha = 2.3 \pm 0.7$ W m^{-2} K^{-1}), given the time-dependent changes in sea surface conditions observed during 1979–2008, than the corresponding coupled atmosphere-ocean general circulation models (AOGCMs) give under constant quadrupled CO$_2$ concentration. These findings help to relieve the apparent contradiction between the larger values of effective climate sensitivity diagnosed from AOGCMs and the smaller values inferred from historical climate change.

1. Introduction

When radiative forcing F (W m^{-2}) is imposed on the climate system, due, for instance, to changes in concentrations of greenhouse gases or other atmospheric components, the resulting global mean surface air temperature change T is determined by the energy budget $F = N + R$, where R is the additional radiation by the climate system to space caused by the perturbation to the climate, and $N = F - R$ is the global mean net downward radiative flux at the top of the atmosphere, which equals the rate of change of the heat content of the climate system and is zero in a steady state. It is usual to write R as αT, so that $N = F - \alpha T$, where the climate feedback parameter α (W m^{-2} K^{-1}) is the increase in radiation to space per unit of global warming. Its reciprocal $s \equiv 1/\alpha$ (K W^{-1} m^2), called the climate sensitivity parameter, is the steady state global warming per unit increase in radiative forcing. Note that negative contributions to α are positive feedbacks on warming, tending to increase the climate sensitivity parameter s.

The separation of radiative forcing from feedback α (or sensitivity s) is convenient if α is a constant property of the climate system and independent of the nature and magnitude of the forcing. However, methods which evaluate α from the energy budget of the climate system using historical estimates of F, N, and T (where by "historical" we mean during the period in which adequate observations of T are available, roughly since the midnineteenth century [e.g., *Gregory et al.*, 2002; *Forest et al.*, 2006; *Forster and Gregory*, 2006; *Aldrin et al.*, 2012; *Huber and Knutti*, 2012; *Otto et al.*, 2013; *Lewis and Curry*, 2015]) tend to give smaller s than exhibited under scenarios of CO$_2$ increase by atmosphere-ocean general circulation models (AOGCMs), which are formulated on the basis of empirical and theoretical understanding to simulate the physical processes of the real world [*Collins et al.*, 2013, Box 12.2]. This difference presents a difficulty in assessing the likely range of s applicable to the future anthropogenic climate change, which is an important quantity because of its implications for many aspects of global and regional climate change which scale approximately with T.

A major reason why α may not be a constant is that the global feedback results from the operation of local feedbacks and is hence sensitive to the spatiotemporal patterns and gradients of change in temperature, cloudiness, snow cover, etc. For example, the pattern of forced climate change may evolve in time, owing to the inherent timescales of response of the climate system, especially in the ocean, yielding a time-dependent α [*Senior and Mitchell*, 2000; *Williams et al.*, 2008; *Held et al.*, 2010; *Armour et al.*, 2013; *Winton et al.*, 2013; *Rose et al.*, 2014; *Andrews et al.*, 2015; *Roe et al.*, 2015]. In abrupt4xCO2 experiments, in which CO$_2$ is instantaneously

quadrupled from its control level at the start and then held constant, α tends to decrease on a decadal timescale in most AOGCMs [*Gregory et al.*, 2004; *Winton et al.*, 2010; *Andrews et al.*, 2012; *Geoffroy et al.*, 2013]. *Andrews et al.* [2015] related this effect to changes in the pattern of warming of sea surface temperature (SST) in the equatorial Pacific and Southern Ocean. By prescribing SST changes from each of two AOGCMs as boundary conditions to its atmosphere GCM (AGCM), they reproduced the time dependence of α in the AOGCM.

Although introduced to describe the response to forcing, α has also been used to quantify the covariation of R and T due to internally generated (unforced) variability of the climate system on interannual and decadal timescales, e.g., El Niño–Southern Oscillation, the Pacific Decadal Oscillation, and the Atlantic Multidecadal Oscillation. Such modes of variability are associated with patterns of surface climate change which differ from those in response to radiative forcing and hence may give different and variable α [*Dessler and Wong*, 2009; *Spencer and Braswell*, 2010; *Colman and Power*, 2010; *Colman and Hanson*, 2013; *Dalton and Shell*, 2013; *Dessler*, 2013; *Brown et al.*, 2014; *Xie et al.*, 2015; *Zhou et al.*, 2015].

In this work, we investigate the behavior of α during the twentieth century, following up the finding of *Andrews* [2014] that the climate sensitivity parameter of HadGEM2-A to the observed SST change of recent decades is less than for abrupt4xCO2. To clarify the subsequent discussion, let us distinguish the climate feedback parameter $\bar{\alpha} = R/T$, as introduced above, and the differential climate feedback parameter $\tilde{\alpha} = dR/dT$ [*Gregory et al.*, 2004]. The former quantity considers the differences of R and T from the unperturbed steady state, whereas the latter describes the covariation of R and T for small changes with respect to the prevailing state. If climate feedback is constant, $\bar{\alpha}$ and $\tilde{\alpha}$ are of course identical. In this work we are mostly concerned with $\tilde{\alpha}$.

2. Climate Sensitivity Parameter With Time-Dependent SST and Sea Ice

We carry out AGCM experiments, denoted "amipPiForcing," in which we prescribe time-varying observationally derived fields of SST and sea ice concentration by interpolation in time from the monthly fields for 1871 to 2010 of the Atmosphere Model Intercomparison Project (AMIP) II data set [*Gates et al.*, 1999; *Taylor et al.*, 2000; *Hurrell et al.*, 2008]. We use the same AGCMs as *Andrews et al.* [2015], viz., HadGEM2-A and HadCM3-A, respectively, the atmosphere components of the HadGEM2-ES [*Collins et al.*, 2011] and HadCM3 [*Gordon et al.*, 2000] AOGCMs. The former contributed to the Coupled Model Intercomparison Project Phase 5 (CMIP5) [*Taylor et al.*, 2012], the latter to the preceding project CMIP3; being a lower resolution and less complex model, HadCM3 is much faster to run. The HadCM3-A amipPiForcing experiment is an ensemble of four integrations from different initial states and the HadGEM2-A an ensemble of two.

In the amipPiForcing experiments, atmospheric composition and all other forcing agents are constant, as for preindustrial conditions (unlike in the CMIP5 protocol for AMIP experiments, discussed later). Hence, F is constant in the energy balance $F = N + \alpha T$. In fact, by the usual definition of forcing with respect to preindustrial, $F = 0 \Rightarrow N = -\alpha T$, $\bar{\alpha} = -N/T$ and $\tilde{\alpha} = -dN/dT$. This situation contrasts with climate change in the real world or an AOGCM driven by increasing time-dependent forcing, when F is balanced by the sum of αT and the ocean heat uptake N. In the AGCM experiment, there is no ocean heat uptake; on the contrary, prescribing the SSTs implies an unlimited ocean heat source which supplies αT to the surface climate to balance the extra heat loss to space as the climate becomes warmer. We assume that α depends only on the sea surface boundary conditions and is unaffected by the absence of the forcing agents. This is an aspect of the general assumption that α is a constant.

In the amipPiForcing experiments, T and N are not constant because the sea surface boundary conditions force the simulated climate system largely to reproduce the time-dependent variations in climate which actually occurred in the historical period (by comparison with the HadCRUT4 observational estimate of *Morice et al.* [2012]; Figure 1a), both the internally generated variability and the response to anthropogenic and natural forcing. Because land surface temperatures are not prescribed, the reproduction of T is not exact, owing to two mechanisms.

First, there is unforced variability over land areas which differs from the historical record and is different between models and observations and among model ensemble members. However, this is small compared with the enforced interannual variability from the SSTs; the intraensemble standard deviation of annual mean T (pooled over years) is 0.037 K in HadGEM2-A and 0.031 K in HadCM3-A, while the interannual standard
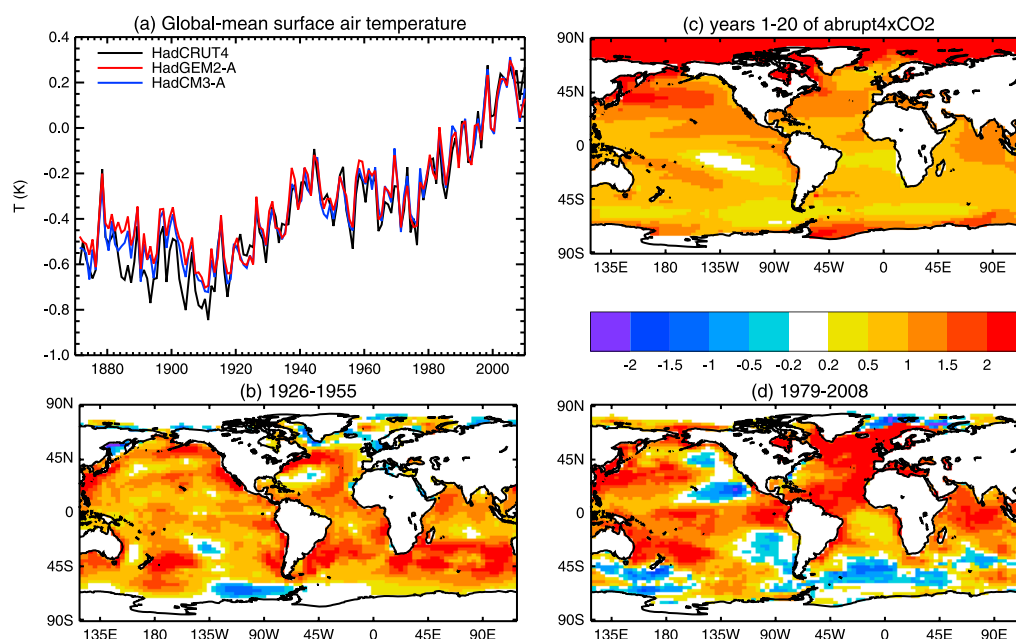
Figure 1. (a) Annual mean global mean surface air temperature change T with respect to the 1979–2008 time mean in HadCRUT4 [*Morice et al.*, 2012] and the ensemble means of the AGCM amipPiForcing experiments. (b, d) Maps of SST patterns $P(\mathbf{x})$ (KK^{-1}), evaluated by regressing annual mean SST against its global mean, for two periods from the AMIP II data set, which have high and low $\tilde{s}$, respectively, in HadCM3-A (Figure 2b); each of these fields has an area average of unity over the sea and was used as a SST perturbation field in a HadCM3-A experiment (Figure 2d). (c) Map of annual mean of the monthly patterns of SST change with respect to control, normalized by the global mean, for years 1–20 of abrupt4xCO2 in HadCM3, used to construct the SST perturbation fields for the HadCM3-A scaledSSTPiForcing experiment.

deviation of T in HadCRUT4, after detrending, is 0.15 K. Therefore, most of the interannual variability would remain in the ensemble mean even if the ensemble were infinitely large, as we discuss again later (section 4).

Second, T increases more over the historical period in the real world than in the amipPiForcing experiments because additional warming over land arises as an adjustment due to changes in CO_2 and other forcing agents [*Folland et al.*, 1998; *Dong et al.*, 2009; *Andrews*, 2014]. (Note that the difference appears to be greatest at the start of the time series in Figure 1a because T is shown relative to the 1979–2008 time mean.) In the amipPiForcing experiment with HadGEM2-A, the increase in T is 85% of what it is in HadCRUT4, and with HadCM3-A the fraction is 89%, according to orthogonal (total least squares) regression of annual mean T from the model against observations, assuming that the observational uncertainty is the same as the model intraensemble standard deviation. Excluding the period before 1910, during which T shows a weak cooling trend, the fractions are 92% and 94%, respectively.

If $\tilde{\alpha} = -\mathrm{d}N/\mathrm{d}T$ is constant, we can estimate it from the slope of the ordinary least squares (OLS) regression of annual means of N against T (Figures 2a and 2b). The use of OLS is consistent with regarding T as an independent variable with no uncertainty, apart from the small contribution from the land area, because we prescribe SST in these experiments. (In section 4 we return to this matter.) The ensembles of regression slopes from individual integrations give similar values for the two models, of $\tilde{\alpha} = 1.72 \pm 0.06$ W m^{-2} K^{-1} for HadGEM2-A and 1.66 ± 0.01 W m^{-2} K^{-1} for HadCM3-A, where the uncertainties are standard errors (the ensemble standard deviation of 0.085 multiplied by $1/\sqrt{2}$ for HadGEM2-A and $0.020/\sqrt{4}$ for HadCM3-A; see section 4 for an alternative approach).

For comparison, regression of annual means for the first 20 years of abrupt4xCO2, during which these models show a linear relationship $N(T)$, gives significantly smaller and distinct values of 0.81 ± 0.09 W m^{-2} K^{-1} for HadGEM2-ES and 1.25 ± 0.04 W m^{-2} K^{-1} for HadCM3 [*Andrews et al.*, 2015]; i.e., $\tilde{s}$ is larger in the abrupt4xCO2 experiments. On longer timescales in abrupt4xCO2, $\tilde{s}$ in these and most other AOGCMs increases [*Andrews et al.*, 2012; *Geoffroy et al.*, 2013; *Andrews et al.*, 2015], increasing the difference from the low sensitivity shown in amipPiForcing. In the AOGCM abrupt4xCO2 experiments, some rapid initial warming of the land as an
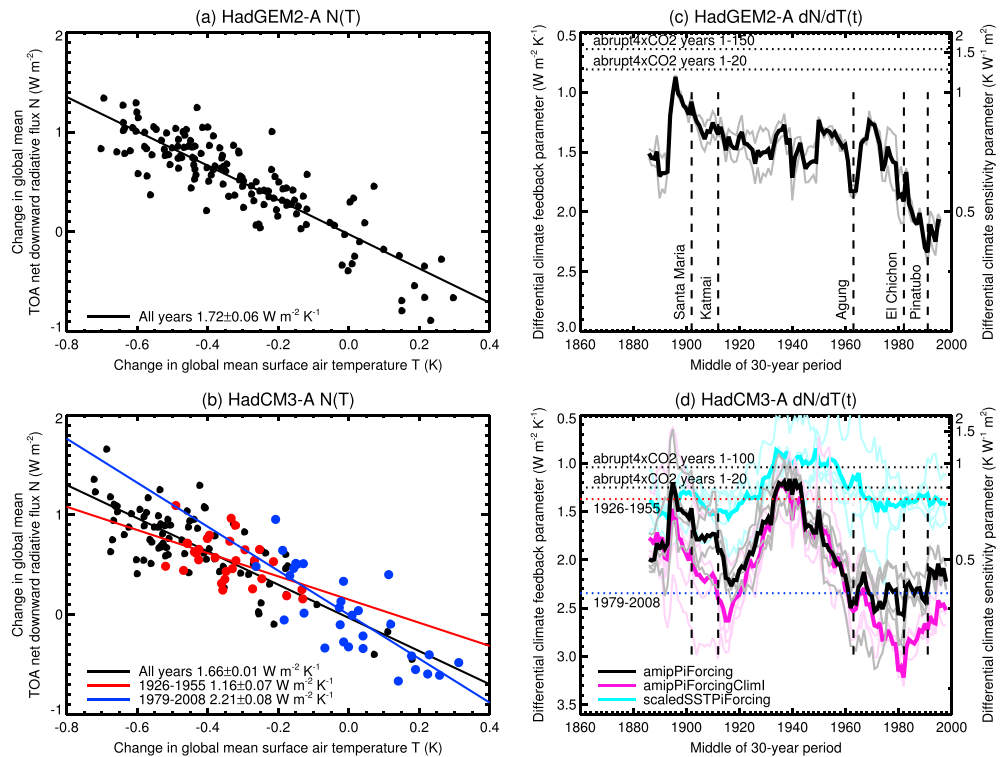
Figure 2. (a, b) Differential climate feedback parameter $\tilde{\alpha}$ evaluated by ordinary least squares regression of annual mean top-of-atmosphere net downward radiation N against T (both expressed as differences from the time mean of the CMIP5 AMIP period 1979–2008) in the amipPiForcing experiments for 1871–2010, and in Figure 2b for the two 30 year periods indicated. The dots indicate ensemble mean annual mean values, the lines the ensemble mean of coefficients from regressions of the individual integrations, with the slope and its standard error shown in the legend. (c, d) Time series of $\tilde{\alpha}$ evaluated by regression in a sliding 30 year window in the amipPiForcing experiments, with amipPiForcingClimI and scaledSSTPiForcing in Figure 2d. Ensemble members are shown with thin lines; the thick lines are the ensemble means of the $\tilde{\alpha}(t)$. The $\tilde{\alpha}$ axis increases downward so that the largest $\tilde{s}$ values are at the top, and the right-hand axis indicates values of $\tilde{s} \equiv 1/\tilde{\alpha}$. To convert to effective climate sensitivity (K), multiply $\tilde{s}$ by 3.4 W m^{-2}, a representative value of $F_{2\times}$. The dotted horizontal lines show $\tilde{\alpha}$ from abrupt4xCO2 experiments [*Andrews et al.*, 2015], and in Figure 2d $\bar{\alpha}$ from experiments with the constant SST perturbations in Figures 1b and 1d for the two 30 year periods indicated in Figure 2b. The dashed vertical lines indicate years of volcanic eruptions, named in Figure 2c.

adjustment to CO_2 occurs within the first year [e.g., *Williams et al.*, 2008; *Andrews et al.*, 2012], but the regression slope in abrupt4xCO2 measures the response of N to global T driven by SST change during years after the initial adjustment and is thus conceptually the same quantity as $\tilde{\alpha}$ from amipPiForcing.

In time-dependent CO_2-forced climate change experiments, it is customary to report the "effective climate sensitivity" (K) [*Murphy*, 1995], which is $sF_{2\times} = F_{2\times}/\alpha$, where $F_{2\times}$ is the effective radiative forcing due to doubling the CO_2 concentration with respect to preindustrial; $F_{2\times}$ is a model-dependent quantity, for which 3.4 Wm^{-2} is a representative value [*Flato et al.*, 2013, Table 9.5]. If α is constant, the effective climate sensitivity equals the equilibrium climate sensitivity, defined as T in a steady state under doubled CO_2 concentration, since a steady state means $N = 0 \Rightarrow T = F_{2\times}/\alpha$. However, α is not constant in nonequilibrium states under CO_2 forcing in most AOGCMs [*Andrews et al.*, 2012]. Therefore, the effective climate sensitivity must be qualified by specifying the scenario and period to which it applies, and caution is needed when comparing estimates of this quantity made from the various kinds of evidence available, including model simulations of the future, observed present-day processes, and past time-dependent climate change. Evaluations of α from palaeoclimate change usually assume a steady state, thus giving estimates of equilibrium climate sensitivity.

The $\tilde{\alpha}$ from amipPiForcing in HadGEM2-A and HadCM3-A corresponds to an effective climate sensitivity of about 2 K, toward the lower end of the likely range of 1.5–4.5 K for equilibrium climate sensitivity in the assessment of *Collins et al.* [2013], and similar to some observationally derived estimates [e.g., *Otto et al.*, 2013]. In contrast, the first 20 years of abrupt4xCO2 give 4.0 K and 3.1 K for HadGEM2-ES and HadCM3, respectively,

in the upper half of the range (using corresponding estimates of $F_{2\times}$ from these models) [*Andrews et al.*, 2015; *Gregory et al.*, 2015]. (Neither of these AOGCMs has been run to a steady state under elevated CO_2, so their equilibrium climate sensitivity is not known.)

3. Time Dependence of the Climate Sensitivity Parameter

We investigate the possibility of time dependence of $\tilde{\alpha}$ by regressing N against T in a sliding 30 year window (Figures 2c and 2d, also showing $\tilde{s} \equiv 1/\tilde{\alpha}$, the differential climate sensitivity parameter $\tilde{s}$). In both models, $\tilde{\alpha}$ exhibits pronounced time variation on multidecadal timescales, whose main features, apparent in all ensemble members, are similar using window lengths of between about 20 and 60 years.

In HadGEM2-A, $\tilde{s}$ is maximum ($\tilde{\alpha}$ is minimum) at the end of the nineteenth century and decreases during the historical period ($\tilde{\alpha}$ increases); this long-term trend is primarily due to changing longwave clear-sky feedback. In HadCM3-A, $\tilde{s}$ has an intervening maximum centred around 1940, which is caused mostly by a temporary change of the contribution to $\tilde{\alpha}$ from cloud radiative effects from about +0.5 W m^{-2} K^{-1} (negative feedback on warming) to −0.5 W m^{-2} K^{-1} (positive feedback, increasing $\tilde{s}$). This midcentury feature is discernible in HadGEM2-A as well but less pronounced; conversely, the long-term trend is weaker in HadCM3-A. The most important points, common to both models, are that $\tilde{\alpha}$ is larger ($\tilde{s}$ is smaller) than its $4 \times CO_2$ value throughout the historical period (except briefly around 1885 and 1940 in HadCM3-A) and that $\tilde{\alpha}$ for recent decades is larger than earlier in the record.

The similar time variation in $\tilde{\alpha}$ among ensemble members of each model, and the features common to both models, can only be caused by the surface boundary conditions. We show that the effect of SST dominates that of sea ice by comparison of HadCM3-A amipPiForcing with a four-member ensemble experiment, denoted "amipPiForcingClimI," having the same SST but with climatological monthly sea ice from the AMIP data set for 1871–1900, i.e., no interannual variation. The time variations of $\tilde{\alpha}$ in amipPiForcingClimI and amipPiForcing are largely consistent (Figure 2d); the differences in the 1910s are due to cloud feedback and since about 1960 due to clear-sky shortwave feedback. Both models show dips in $\tilde{s}$ around the times of the explosive volcanic eruptions of Agung, El Chichon, and Pinatubo, which caused climatic cooling due to forcing by stratospheric aerosol. Since time-dependent volcanic stratospheric aerosol, like other radiative forcing agents, is not included in the AGCM simulations, the variation of $\tilde{s}$ must be due to the effect on patterns of SST.

Let us assume that α is a function of $P(\mathbf{x})$, which is the spatial pattern of SST change (KK^{-1}) obtained by regression of annual mean SST$(\mathbf{x}, t)$, where $\mathbf{x}$ is geographical location and t is year, against global mean annual mean SST(t). We evaluate P for 1926–1955 and 1979–2008 from the AMIP II data set (Figures 1b and 1d). During these 30 year periods $\tilde{\alpha}$ in HadCM3-A was, respectively, small and large (1.16 ± 0.07 W m^{-2} K^{-1} and 2.21 ± 0.08 W m^{-2} K^{-1}, shown in Figure 2b), which are significantly different at the 5% level. By construction, each P field has an area average of unity (over the sea). We add each P field (in K, i.e., the field of SST change for a 1 K area average warming) to every monthly field in the annual cycle of climatological mean SST from the AMIP II data set for 1871–1900. Using each of the two perturbed SST climatologies with climatological mean monthly sea ice for 1871–1900, i.e., having no interannual variation in sea surface conditions, we carry out a 30 year integration of HadCM3-A. The control for these two experiments is a 30 year integration with the 1871–1900 climatological monthly sea ice and unperturbed SST (as if $P = 0$ everywhere).

For each P field, we estimate $\overline{\alpha} = -N/T$ from the 30 year mean changes in N and T with respect to the control, and the values thus obtained are in good agreement with those from $\tilde{\alpha}$ in the corresponding periods of the time-dependent amipPiForcing integrations (Figure 2d), confirming that the variation in $\tilde{\alpha}$ is due to the patterns of SST change. A notable difference between these patterns (Figures 1b and 1d) is the cooling in 1979–2008 in the east Pacific, in regions where marine stratocumulus low cloud is generally thought to make a positive contribution to climate sensitivity when the SST warms with the global mean [*Boucher et al.*, 2013]. The reversal of the sign of the contribution from these regions to the global mean during 1979–2008 could be part of the explanation for the low global sensitivity.

For both periods $\overline{\alpha}$ is larger than $\tilde{\alpha}$ in abrupt4xCO2. We demonstrate that this is due to the SST patterns by carrying out a four-member ensemble experiment, denoted "scaledSSTPiForcing," with preindustrial atmospheric composition, climatological monthly sea ice for 1871–1900, and monthly SST fields constructed by the pattern-scaling method of *Andrews et al.* [2015, section 4b]. We calculate monthly mean fields of climatological SST change with respect to preindustrial control for years 1–20 of abrupt4xCO2 in HadCM3,

each divided by its global mean (giving a pattern in KK^{-1} with unit mean). The annual mean pattern has no substantially negative areas (Figure 1c), like the similar field shown by *Andrews et al.* [2015, Figure 5a] for the CMIP5 ensemble mean. We scale the monthly patterns by the monthly time series of HadCRUT4 *T* anomaly with respect to the climatological mean of 1871–1900 and add them to the AMIP II climatological SST fields for 1871–1900. Thus, we obtain SST fields whose global mean varies as observed historically but with the geographical pattern of response to quadrupled CO_2 forcing in HadCM3.

The $\tilde{\alpha}$ of scaledSSTPiForcing has no trend and varies on decadal time series around the $\tilde{\alpha}$ of HadCM3 abrupt4xCO2 years 1–20, from which the SST patterns were constructed (Figure 2d). It is thus consistently smaller ($\tilde{s}$ larger) than in amipPiForcing, mainly because cloud radiative effects give a small net positive feedback on warming (negative contribution to α) in scaledSSTPiForcing but a generally negative feedback in amipPiForcing. This is opposite to the finding of *Zhou et al.* [2015] in CMIP5 AOGCMs, where cloud feedbacks give a weaker positive feedback for CO_2-forced climate change than for unforced variability, the difference also being attributed to SST patterns.

Since the SST patterns are the same in the amipPiForcing experiments with the two AGCMs but the outcome is model dependent (Figures 2c and 2d), $\tilde{\alpha}$ must also depend on the atmospheric feedbacks in each model. We expect such dependence from much previous work in which the same SST perturbation has been prescribed in a range of models [e.g., *Cess et al.*, 1996; *Ringer et al.*, 2014].

The two AGCMs agree on a value of $\tilde{\alpha} \simeq 2.0$ W m^{-2} K^{-1} ($\tilde{s} \simeq 0.5$ K W^{-1} m^2) for 1979–2008. In standard CMIP5 AMIP experiments, AGCMs are integrated with historical SSTs for this period. Unlike amipPiForcing, the AMIP experiments have time-dependent forcing agents. Since $F = N + \alpha T$, we can evaluate $\tilde{\alpha}$ by regressing annual mean $F - N$ against T [*Forster and Gregory*, 2006; *Tett et al.*, 2007], using the historical effective radiative forcing $F(t)$ from the assessment of *Myhre et al.* [2013]. (We have repeated the calculations using $F(t)$ from *Andrews* [2014], with the same qualitative conclusions and only small quantitative differences.) Across the ensemble of 19 AGCMs, the mean and standard deviation of $\tilde{\alpha}$ are 2.3 ± 0.7 W m^{-2} K^{-1} ($\tilde{s} = 0.46 \pm 0.13$ K W^{-1} m^2) for 1979–2008 (distributions shown in Figure S1 in the supporting information). The corresponding AOGCMs give $\tilde{\alpha} = 1.0 \pm 0.3$ W m^{-2} K^{-1} ($\tilde{s} = 1.0 \pm 0.3$ K W^{-1} m^2) in years 1–150 of abrupt4xCO2 (following *Andrews et al.* [2012]). Thus, HadGEM2-ES and HadCM3 are typical of the CMIP5 ensemble in indicating a lower $\tilde{s}$ for SST changes observed in recent decades than predicted in response to CO_2 increase.

4. Discussion

Our results suggest that the differential climate feedback parameter $\tilde{\alpha}$ varied on multidecadal timescales during the historical period and that it was generally larger than for abrupt4xCO2, in particular, during the last three decades. In order to interpret these findings, we need to consider the influences on the relationship between N and T, from which we determine $\tilde{\alpha}$.

Different geographical patterns of SST that produce the same global mean T can give different N; for instance, *Andrews et al.* [2015] show a case where changing the pattern of SST alters N without changing T (the rapid SST adjustment to quadrupling CO_2). In addition, there is variability in N internally generated by the atmosphere-land system. Including both of these phenomena, we may write $N_i(t) = -\overline{\alpha}T(t) + N'(t) + \epsilon_i(t)$ in a amipPiForcing integration, where i is the ensemble member number, $\overline{\alpha}$ is determined by the time mean pattern of SST change (whose amplitude increases as forced climate change grows in magnitude), $N'(t)$ is the contribution that depends on interannual variation or trends in the pattern of SST, and $\epsilon_i(t)$ is variability that is not forced by SST and therefore different in each ensemble member. We may alternatively write this as $N_i(t) = -\tilde{\alpha}(t)T(t) + \epsilon_i(t)$, with time-dependent $\tilde{\alpha}(t) = \overline{\alpha} - N'(t)/T(t)$.

The estimated $\tilde{\alpha}$ from the ensemble of regression slopes of N against T in individual amipPiForcing integrations (reported in section 2) is 1.72 ± 0.06 W m^{-2} K^{-1} for HadGEM2-A and 1.66 ± 0.01 for HadCM3-A (mean and standard error). Alternatively, from regression of the ensemble mean N against T, we obtain 1.74 ± 0.08 W m^{-2} K^{-1} and 1.67 ± 0.09 for the two models. The means are similar from the two methods, but the standard error from the ensemble mean regression is larger.

If $N'(t)$ was zero, the scatter around the regression line would be caused only by $\epsilon_i(t)$, which is different in each ensemble member i. In that case, the standard error from the ensemble mean regression would decrease with $1/\sqrt{M}$, where M is the size of the ensemble, just as the standard error estimated from the ensemble of individual regressions does (formula in Appendix A in the supporting information). Actually, it does not

decrease so much because most of the scatter is due to $N'(t)$ caused by SST variation, which is the same in every ensemble member. This contradicts the assumption made in deriving the OLS standard error, that the scatter is due to uncertainty in N which is independent of SST and can therefore be estimated from the residual of the fit. To clarify this, consider the special case of $\epsilon(t) = 0$. All the realisations will be identical, so the standard error estimated from the spread of regression slopes will be zero, but N' will cause a residual deviation from the regression line and, hence, a nonzero standard error of the ensemble mean slope.

The OLS regression minimizes the root-mean-square residual, giving the best choice of $\tilde{\alpha}$ to describe the relationship between $R=-N$, the increased radiation to space, and the SST change which causes it. However, this minimum residual is large, because constant α is not an accurate assumption, and the scatter is caused mostly by the variation in $\tilde{\alpha}$. The small standard errors from the ensemble of slopes indicate that the time dependence of $\tilde{\alpha}$ is robust in each model, given the observed time dependence of the SST patterns. For the cause of the latter, we consider three possibilities, which may all apply.

The first possibility is that unforced variability could have a strong influence on historical variation in the patterns of SST and hence on $\tilde{\alpha}$. This possibility is suggested by studies of the spatiotemporal variation of temperature change with reference to the recent hiatus in T [Dai et al., 2015; Xie et al., 2015]. It implies that $\tilde{\alpha}$ evaluated from a short period may not be applicable to forced climate change [Dessler, 2013; Zhou et al., 2015], and using the entire observed historical record will yield the best estimate of $\tilde{\alpha}$ for the response to forcing by minimizing the influence of long-period variability. That the historical $\tilde{\alpha}$ is larger (sensitivity smaller) than expected for the response to forcing would be explained if patterns of unforced variability in SST generally result in larger $\tilde{\alpha}$, and the observed record is not long enough to remove this effect.

The second possibility is that the time dependence in historical $\tilde{\alpha}$ could arise from a nonlinear response of the SST patterns to the magnitude of the forcing or of climate feedback processes to the amplitude of the forced SST pattern. In HadCM3 [Good et al., 2012; Gregory et al., 2015] and CCSM3 [Jonko et al., 2012], $\tilde{s}$ for CO_2 forcing rises with CO_2 concentration. If this is so in reality, given that the present CO_2 concentration is about $1.5\times$ preindustrial, the historical $\tilde{s}$ would be smaller ($\tilde{\alpha}$ larger) than the sensitivity to $4 \times CO_2$. However, the trend in HadGEM2-A goes in the opposite sense, toward smaller $\tilde{s}$ as time passes.

The third possibility is that the patterns of SST change and, hence, $\tilde{\alpha}$ might vary during the amipPiForcing experiment because of changes in relative importance of the various forcing agents, which have different spatiotemporal "fingerprints" [Bindoff et al., 2013]. For example, $\tilde{s}$ might be smaller during recent decades because of the effect of strong volcanic forcing on SST patterns, although this would not explain larger $\tilde{s}$ in the late nineteenth century (Figures 2c and 2d). Since amipPiForcing does not include forcing agents, their influence on $\tilde{\alpha}$ can come only through their effect on historical SST, not directly through the tropospheric energy balance.

Tropospheric anthropogenic aerosol exerts a negative and particularly heterogeneous radiative forcing, which may partly have driven variations in the patterns of SST in the Atlantic and Pacific [e.g., Booth et al., 2012; Allen et al., 2015; Boo et al., 2015]. Its global mean magnitude has increased less rapidly or stabilized since the 1970s [Gregory and Forster, 2008; Boucher et al., 2013; Regayre et al., 2014; Rotstayn et al., 2015]. There is some evidence that α for this forcing is about 40% smaller (s 40% larger) than for well-mixed greenhouse gases [Shindell, 2014; Kummer and Dessler, 2014; Rotstayn et al., 2015], though this depends on how the forcing is evaluated [Paynter and Frölicher, 2015; Marvel et al., 2016]. This would make the net s during the historical period smaller than for CO_2 alone (Appendix B in the supporting information), but the decreasing ratio of the magnitude of the (net negative) anthropogenic aerosol forcing to the magnitude of other anthropogenic forcings (net positive, especially from greenhouse gases) implies an increasing net climate sensitivity parameter over recent decades (and into the future), the opposite trend to the amipPiForcing experiments.

5. Conclusions

It is evident that both forced response and unforced variability can affect the patterns of SST change and hence $\tilde{\alpha}$. Our models agree on historical $\tilde{\alpha} \simeq 1.7 \, \mathrm{W \, m^{-2} \, K^{-1}}$ (effective climate sensitivity of about 2 K) for the historical period as a whole, i.e., smaller effective climate sensitivity than for $4 \times CO_2$, and they agree with other AMIP models that $\tilde{\alpha} \simeq 2.2 \, \mathrm{W \, m^{-2} \, K^{-1}}$ (effective climate sensitivity of about 1.5 K) for 1979–2008. Coincidentally, these recent decades, in which we have most observational information, especially from satellite and ocean observation, have $\tilde{\alpha}$ which is markedly larger than for the historical period in general.

Both of our models show time variation in $\tilde{\alpha}$, but the similarities in the details are limited, indicating a large influence from their different representations of feedbacks. The trends in $\tilde{\alpha}$ in the amipPiForcing simulations are not consistent with the expected effects of increasing CO_2 concentration and the declining fraction of anthropogenic forcing due to tropospheric aerosol, which may imply that unforced or naturally forced variability is more important and produces a larger $\tilde{\alpha}$, but our results do not support a clear conclusion about which influences are dominant. Further research into this issue is called for.

The Cloud Feedback Model Intercomparison Project of CMIP6, the successor to CMIP5, includes the amipPiForcing experiment and various other AGCM experiments with different fixed patterns of SST change, while the Radiative Forcing Model Intercomparison Project will diagnose $F(t)$ in AOGCMs, so that it will be possible to estimate $\tilde{\alpha}$ consistently in AOGCM historical experiments from $F - N$ and T. It would be informative also to carry out AGCM experiments using sea surface conditions from AOGCM experiments with individual forcing agents for comparison with $\tilde{\alpha}$ calculated from N and T in the absence of the forcing agent. These new experiments will show whether other AGCMs exhibit variation like ours do in the climate sensitivity parameter during the historical period and will allow analysis to identify the feedback mechanisms responsible for the dependence on patterns of SST change, such as the low climate sensitivity parameter of recent decades indicated by the CMIP5 AMIP simulations.

If CMIP6 results corroborate our finding that the climate sensitivity parameter indicated by GCMs under large CO_2 increases is greater than for historical SST change simulated by the same GCMs, it would help to relieve the apparent contradiction between the different sources of evidence that have been used to assess the effective climate sensitivity. Further investigation would be needed to explain the difference, for which some possible explanations are that the climate sensitivity parameter for CO_2 forcing is underestimated from observed climate change because of a large influence from unforced variability, that it is overestimated by GCMs, or that it cannot easily be inferred from observed climate change because of the time-dependent relative importance of various forcing agents.

References

Aldrin, M., M. Holden, P. Guttorp, R. B. Skeie, G. Myhre, and T. K. Berntsen (2012), Bayesian estimation of climate sensitivity based on a simple climate model fitted to observations of hemispheric temperatures and global ocean heat content, *Environmetrics*, *23*, 253–271, doi:10.1002/env.2140.

Allen, R. J., J. R. Norris, and M. Kovilakam (2015), Influence of anthropogenic aerosols and the Pacific Decadal Oscillation on tropical belt width, *Nat. Geosci.*, *7*, 270–274, doi:10.1038/ngeo2091.

Andrews, T. (2014), Using an AGCM to diagnose historical effective radiative forcing and mechanisms of recent decadal climate change, *J. Clim.*, *27*, 1193–1209, doi:10.1175/jcli-d-13-00336.1.

Andrews, T., J. M. Gregory, M. J. Webb, and K. E. Taylor (2012), Forcing, feedbacks and climate sensitivity in CMIP5 coupled atmosphere-ocean climate models, *Geophys. Res. Lett.*, *39*, L09712, doi:10.1029/2012GL051607.

Andrews, T., J. M. Gregory, and M. J. Webb (2015), The dependence of radiative forcing and feedback on evolving patterns of surface temperature change in climate models, *J. Clim.*, *28*, 1630–1648, doi:10.1175/jcli-d-14-00545.1.

Armour, K. C., C. M. Bitz, and G. H. Roe (2013), Time-varying climate sensitivity from regional feedbacks, *J. Clim.*, *26*, 4518–4534, doi:10.1175/jcli-d-12-00544.1.

Bindoff, N. L., et al. (2013), Detection and attribution of climate change: From global to regional, in *Climate Change 2013: The Physical Science Basis. Contribution of Working Group I to the Fifth Assessment Report of the Intergovernmental Panel on Climate Change*, edited by T. F. Stocker et al., pp. 867–952, Cambridge Univ. Press, Cambridge, U. K., and New York, doi:10.1017/cbo9781107415324.022.

Boo, K.-O., B. B. B. Booth, Y.-H. Byun, J. Lee, C. Cho, S. Shim, and K.-T. Kim (2015), Influence of aerosols in multidecadal SST variability simulations over the North Pacific, *J. Geophys. Res. Atmos.*, *120*, 517–531, doi:10.1002/2014JD021933.

Booth, B. B. B., N. J. Dunstone, P. R. Halloran, T. Andrews, and N. Bellouin (2012), Aerosols implicated as a prime driver of twentieth-century North Atlantic climate variability, *Nature*, *484*, 228–232, doi:10.1038/nature10946.

Boucher, O., et al. (2013), Clouds and aerosols, in *Climate Change 2013: The Physical Science Basis. Contribution of Working Group I to the Fifth Assessment Report of the Intergovernmental Panel on Climate Change*, edited by T. F. Stocker et al., pp. 571–657, Cambridge Univ. Press, Cambridge, U. K., and New York, doi:10.1017/cbo9781107415324.016.

Brown, P. T., W. Li, L. Li, and Y. Ming (2014), Top-of-atmosphere radiative contribution to unforced decadal global temperature variability in climate models, *Geophys. Res. Lett.*, *41*, 5175–5183, doi:10.1002/2014GL060625.

Cess, R. D., et al. (1996), Cloud feedback in atmospheric general circulation models: An update, *J. Geophys. Res.*, *101*, 12,791–12,794.

Collins, M., et al. (2013), Long-term climate change: Projections, commitments and irreversibility, in *Climate Change 2013: The Physical Science Basis. Contribution of Working Group I to the Fifth Assessment Report of the Intergovernmental Panel on Climate Change*, edited by M. Collins et al., pp. 1029–1136, Cambridge Univ. Press, doi:10.1017/cbo9781107415324.024.

Collins, W. J., et al. (2011), Development and evaluation of an Earth-system model—HadGEM2, *Geosci. Model Devel.*, *4*, 1051–1075, doi:10.5194/gmd-4-1051-2011.

Colman, R. A., and L. I. Hanson (2013), On atmospheric radiative feedbacks associated with climate variability and change, *Clim. Dyn.*, *40*, 475–492, doi:10.1007/s00382-012-1391-3.

Colman, R. A., and S. B. Power (2010), Atmospheric radiative feedbacks associated with transient climate change and climate variability, *Clim. Dyn.*, *34*, 919–933, doi:10.1007/s00382-009-0541-8.

Dai, A., J. C. Fyfe, S.-P. Xie, and X. Dai (2015), Decadal modulation of global surface temperature by internal climate variability, *Nat. Clim. Change*, *5*, 555–559, doi:10.1038/nclimate2605.

Dalton, M. M., and K. M. Shell (2013), Comparison of short-term and long-term radiative feedbacks and variability in twentieth-century global climate model simulations, *J. Clim.*, *26*, 10,051–10,070, doi:10.1175/jcli-d-12-00564.1.

Dessler, A. E. (2013), Observations of climate feedbacks over 2000-10 and comparisons to climate models, *J. Clim.*, *26*, 333–342, doi:10.1175/jcli-d-11-00640.1.

Dessler, A. E., and S. Wong (2009), Estimates of the water vapor climate feedback during El Niño–Southern Oscillation, *J. Clim.*, *22*, 6404–6412, doi:10.1175/2009jcli3052.1.

Dong, B., J. M. Gregory, and R. Sutton (2009), Understanding land-sea warming contrast in response to increasing greenhouse gases. Part I: Transient adjustment, *J. Clim.*, *22*, 3079–3097, doi:10.1175/2009jcli2652.1.

Flato, G., et al. (2013), Evaluation of climate models, in *Climate Change 2013: The Physical Science Basis. Contribution of Working Group I to the Fifth Assessment Report of the Intergovernmental Panel on Climate Change*, edited by G. Flato et al., pp. 741–882, Cambridge Univ. Press, doi:10.1017/cbo9781107415324.020.

Folland, C. K., D. M. H. Sexton, D. J. K. Karoly, C. E. Johnson, D. P. Rowell, and D. E. Parker (1998), Influences of anthropogenic and oceanic forcing on recent climate change, *Geophys. Res. Lett.*, *25*, 353–356.

Forest, C. E., P. H. Stone, and A. P. Sokolov (2006), Estimated PDFs of climate system properties including natural and anthropogenic forcings, *Geophys. Res. Lett.*, *33*, L01705, doi:10.1029/2005GL023977.

Forster, P. M. D. F., and J. M. Gregory (2006), The climate sensitivity and its components diagnosed from Earth radiation budget data, *J. Clim.*, *19*, 39–52.

Gates, W. L., et al. (1999), An overview of the results of the Atmospheric Model Intercomparison Project (AMIP I), *Bull. Am. Meteorol. Soc.*, *80*, 29–55.

Geoffroy, O., D. Saint-Martin, G. Bellon, A. Voldoire, D. J. L. Olivié, and S. Tytéca (2013), Transient climate response in a two-layer energy-balance model. Part II: Representation of the efficacy of deep-ocean heat uptake and validation for CMIP5 AOGCMs, *J. Clim.*, *26*, 1859–1876, doi:10.1175/jcli-d-12-00196.1.

Good, P., W. Ingram, F. H. Lambert, J. A. Lowe, J. M. Gregory, M. J. Webb, M. A. Ringer, and P. Wu (2012), A step-response approach for predicting and understanding non-linear precipitation changes, *Clim. Dyn.*, *39*, 2789–2803, doi:10.1007/s00382-012-1571-1.

Gordon, C., C. Cooper, C. A. Senior, H. Banks, J. M. Gregory, T. C. Johns, J. F. B. Mitchell, and R. A. Wood (2000), The simulation of SST, sea ice extents and ocean heat transports in a version of the Hadley Centre coupled model without flux adjustments, *Clim. Dyn.*, *16*, 147–168, doi:10.1007/s003820050010.

Gregory, J. M., and P. M. Forster (2008), Transient climate response estimated from radiative forcing and observed temperature change, *J. Geophys. Res.*, *113*, D23105, doi:10.1029/2008JD010405.

Gregory, J. M., R. J. Stouffer, S. C. B. Raper, P. A. Stott, and N. A. Rayner (2002), An observationally based estimate of the climate sensitivity, *J. Clim.*, *15*, 3117–3121, doi:10.1175/1520-0442(2002)015<3117:aobeot>2.0.co;2.

Gregory, J. M., W. J. Ingram, M. A. Palmer, G. S. Jones, P. A. Stott, R. B. Thorpe, J. A. Lowe, T. C. Johns, and K. D. Williams (2004), A new method for diagnosing radiative forcing and climate sensitivity, *Geophys. Res. Lett.*, *31*, L03205, doi:10.1029/2003GL018747.

Gregory, J. M., T. Andrews, and P. Good (2015), The inconstancy of the transient climate response parameter under increasing CO_2, *Philos. Trans. R. Soc. London*, *373*, 20140417, doi:10.1098/rsta.2014.0417.

Held, I. M., M. Winton, K. Takahashi, T. Delworth, F. Zeng, and G. K. Vallis (2010), Probing the fast and slow components of global warming by returning abruptly to preindustrial forcing, *J. Clim.*, *23*, 2418–2427, doi:10.1175/2009jcli3466.1.

Huber, M., and R. Knutti (2012), Anthropogenic and natural warming inferred from changes in Earth's energy balance, *Nat. Geosci.*, *5*, 31–36, doi:10.1038/ngeo1327.

Hurrell, J. W., J. J. Hack, D. Shea, J. M. Caron, and J. Rosinski (2008), A new sea surface temperature and sea ice boundary dataset for the Community Atmosphere Model, *J. Clim.*, *21*, 5145–5153, doi:10.1175/2008jcli2292.1.

Jonko, A. K., K. M. Shell, B. M. Sanderson, and G. Danabasoglu (2012), Climate feedbacks in CCSM3 under changing CO_2 forcing. Part II: Variation of climate feedbacks and sensitivity with forcing, *J. Clim.*, *26*, 2784–2795, doi:10.1175/jcli-d-12-00479.1.

Kummer, J. R., and A. E. Dessler (2014), The impact of forcing efficacy on the equilibrium climate sensitivity, *Geophys. Res. Lett.*, *41*, 3565–3568, doi:10.1002/2014GL060046.

Lewis, N., and J. A. Curry (2015), The implications for climate sensitivity of AR5 forcing and heat uptake estimates, *Clim. Dyn.*, *45*, 1009–1023, doi:10.1007/s00382-014-2342-y.

Marvel, K., G. A. Schmidt, R. L. Miller, and L. S. Nazarenko (2016), Implications for climate sensitivity from the response to individual forcings, *Nat. Clim. Change*, *6*(4), 386–389, doi:10.1038/nclimate2888.

Morice, C. P., J. J. Kennedy, N. A. Rayner, and P. D. Jones (2012), Quantifying uncertainties in global and regional temperature change using an ensemble of observational estimates: The HadCRUT4 data set, *J. Geophys. Res.*, *117*, D08101, doi:10.1029/2011JD017187.

Murphy, J. M. (1995), Transient response of the Hadley Centre coupled ocean-atmosphere model to increasing carbon dioxide: Part III. Analysis of global-mean response using simple models, *J. Clim.*, *8*, 496–514.

Myhre, G., et al. (2013), Anthropogenic and natural radiative forcing, in *Climate Change 2013: The Physical Science Basis. Contribution of Working Group I to the Fifth Assessment Report of the Intergovernmental Panel on Climate Change*, edited by G. Myhre et al., pp. 659–740, Cambridge Univ. Press, Cambridge, U. K., and New York, doi:10.1017/cbo9781107415324.018.

Otto, A., et al. (2013), Energy budget constraints on climate response, *Nat. Geosci.*, *6*, 415–416, doi:10.1038/ngeo1836.

Paynter, D., and T. L. Frölicher (2015), Sensitivity of radiative forcing, ocean heat uptake, and climate feedback to changes in anthropogenic greenhouse gases and aerosols, *J. Geophys. Res. Atmos.*, *120*, 9837–9854, doi:10.1002/2015JD023364.

Regayre, L. A., K. J. Pringle, B. B. B. Booth, L. A. Lee, G. W. Mann, J. Browse, M. T. Woodhouse, A. Rap, C. L. Reddington, and K. S. Carslaw (2014), Uncertainty in the magnitude of aerosol-cloud radiative forcing over recent decades, *Geophys. Res. Lett.*, *41*, 9040–9049, doi:10.1002/2014GL062029.

Ringer, M. A., T. Andrews, and M. J. Webb (2014), Global-mean radiative feedbacks and forcing in atmosphere-only and coupled atmosphere-ocean climate change experiments, *Geophys. Res. Lett.*, *41*, 4035–4042, doi:10.1002/2014GL060347.

Roe, G. H., N. Feldl, K. C. Armour, Y.-T. Hwang, and D. M. W. Frierson (2015), The remote impacts of climate feedbacks on regional climate predictability, *Nat. Geosci.*, *8*, 135–139, doi:10.1038/ngeo2346.

Rose, B. E. J., K. C. Armour, D. S. Battisti, N. Feldl, and D. D. B. Koll (2014), The dependence of transient climate sensitivity and radiative feedbacks on the spatial pattern of ocean heat uptake, *Geophys. Res. Lett.*, *41*, 1071–1078, doi:10.1002/2013GL058955.

Rotstayn, L. D., M. A. Collier, D. T. Shindell, and O. Boucher (2015), Why does aerosol forcing control historical global-mean surface temperature change in CMIP5 models?, *J. Clim.*, *28*, 6608–6625, doi:10.1175/jcli-d-14-00712.1.

Senior, C. A., and J. F. B. Mitchell (2000), The time dependence of climate sensitivity, *Geophys. Res. Lett.*, *27*, 2685–2688.

Shindell, D. (2014), Inhomogeneous forcing and transient climate sensitivity, *Nat. Clim. Change*, *4*, 274–277, doi:10.1038/nclimate2136.

Spencer, R. W., and W. D. Braswell (2010), On the diagnosis of radiative feedback in the presence of unknown radiative forcing, *J. Geophys. Res.*, *115*, D16109, doi:10.1029/2009JD013371.

Taylor, K. E., D. Williamson, and F. Zwiers (2000), The sea surface temperature and sea ice concentration boundary conditions for AMIP II simulations, *PCMDI Rep. 60*, Lawrence Livermore National Laboratory, Program for Climate Model Diagnosis and Intercomparison, Livermore.

Taylor, K. E., R. J. Stouffer, and G. A. Meehl (2012), An overview of CMIP5 and the experiment design, *Bull. Am. Meteorol. Soc.*, *93*, 485–498, doi:10.1175/bams-d-11-00094.1.

Tett, S. F. B., R. Betts, T. J. Crowley, J. Gregory, T. C. Johns, A. Jones, T. J.Osborn, E. Öström, D. L. Roberts, and M. J. Woodage (2007), The impact of natural and anthropogenic forcings on climate and hydrology, *Clim. Dyn.*, *28*, 3–34, doi:10.1007/s00382-006-0165-1.

Williams, K. D., W. J. Ingram, and J. M. Gregory (2008), Time variation of effective climate sensitivity in GCMs, *J. Climate*, *21*, 5076–5090, doi:10.1175/2008jcli2371.1.

Winton, M., K. Takahashi, and I. M. Held (2010), Importance of ocean heat uptake efficacy to transient climate change, *J. Clim.*, *23*, 2333–2344, doi:10.1175/2009jcli3139.1.

Winton, M., S. M. Griffies, B. L. Samuels, J. L. Sarmiento, and T. L. Frölicher (2013), Connecting changing ocean circulation with changing climate, *J. Clim.*, *26*, 2268–2278, doi:10.1175/jcli-d-12-00296.1.

Xie, S.-P., Y. Kosaka, and Y. M. Okumura (2015), Distinct energy budgets for anthropogenic and natural changes during global warming hiatus, *Nat. Geosci.*, doi:10.1038/ngeo2581.

Zhou, C., M. D. Zelinka, A. E. Dessler, and S. A. Klein (2015), The relationship between interannual and long-term cloud feedbacks, *Geophys. Res. Lett.*, *42*, 10,463–10,469, doi:10.1002/2015GL066698.